*Journal of Naval Architecture and Marine Engineering*
*December, 2023*
http://dx.doi.org/10.3329/jname.v20.i3.69990 *http://www.banglajol.info*

# NUMERICAL INVESTIGATION OF HYDRODYNAMIC PERFORMANCE OF CONVENTIONAL AND DUCTED PROPELLERS

**M. S. Tarafder[1], M. I. Haque[2*], M. Asaduzzaman[3], M. Z. I. Laku[4]**

[1]Department of Naval Architecture and Marine Engineering, Bangladesh University of Engineering and Technology, Dhaka, mshahjadatarafder@name.buet.ac.bd
[2*]Department of Naval Architecture and Marine Engineering, Bangladesh University of Engineering and Technology, Dhaka, imdadulhaque@name.buet.ac.bd
[3]Department of Naval Architecture and Marine Engineering, Bangladesh University of Engineering and Technology, Dhaka, asadshipon.14@gmail.com
[4]Department of Naval Architecture and Marine Engineering, Bangladesh University of Engineering and Technology, Dhaka, zahidlaku72@gmail.com

## Abstract:

*An efficient and optimized propeller can reduce ship operating costs substantially. The recent development of Computational Fluid Dynamics (CFD) has a significant impact on the initial stage of propeller design. Being motivated by the success of a CFD approach known as Reynolds Averaged Navier-Stokes Equation (RANSE) in solving many hydrodynamic problems, this paper explores the use of RANSE solver to estimate propeller open water characteristics. Multiple RANSE solvers can be used for CFD simulation. Among these k-$\epsilon$ turbulence model is used for its better performance on propeller analysis. Numerical results are compared with the results obtained from well-established polynomial regression formulae of Wageningen-B series propeller. A comparison shows an error of less than 5% for most of the cases. The same propeller is numerically analyzed again after fitting a 19A duct on it. To achieve optimal performance space between the duct and propeller blade tip is kept as small as possible. Grid independence test is done in both cases for a more accurate estimation within a particular time frame. Mesh sensitivity analysis is carried out in this paper based on thrust and torque coefficients. This paper shows that the maximum computed efficiencies for both the conventional and ducted propeller systems are found to be 60% but at different speeds. The ducted propeller system gives better performance up to advance coefficient J=0.48.*

***Keywords:*** Computational fluid dynamics; propeller analysis; ducted propeller; RANSE solver.

**NOMENCLATURE**

| | | | |
|---|---|---|---|
| $K_T$ | thrust coefficient | $\eta_0$ | open water efficiency |
| $K_Q$ | torque coefficient | $\omega$ | angular velocity |
| $\frac{P}{D}$ | pitch ratio | $\rho$ | water density |
| $\frac{A_E}{A_0}$ | expanded blade area ratio | $\varepsilon$ | turbulent dissipation |
| $V_A$ | speed of advance | $\mu_t$ | turbulent viscosity |
| $Z$ | number of blades | $\mu$ | dynamic viscosity |
| $J$ | advance ratio | $Q$ | torque |
| $n$ | propeller revolution rate | $k$ | turbulent kinetic energy |
| $D$ | propeller diameter | $u, v, w$ | velocity components |
| $T$ | thrust | $p$ | pressure |

***Greek symbols***

## 1. Introduction

The present maritime industry is substantially more competitive than it was before (Midoro *et al*, 2005). To survive in the industry by achieving high speed and low power consumption an optimized and efficient propeller design

1813-8535 (Print), 2070-8998 (Online)  Selected from papers presented at MARTEC 2022

is far more important now. Traditional propeller design is experiment-based. This requires a higher cost and a significant amount of time. However, thanks to the quick advancement of computer tools, computational fluid dynamics (CFD) techniques may now be used to quickly handle a variety of hydrodynamic issues. There are numerous techniques to using CFD programs to estimate propeller open water parameters inside the CFD methodology. These include the Reynolds Averaged Navier-Stokes Equation, Surface Panel Methods, Lifting Line Theory, Blade-Element Theory, and Boundary Element Methods (RANSE) (Perali *et al*, 2016). RANSE is the most popular among these because it is more similar to actual fluid flow around the propeller. But it costs more and takes longer time to calculate. In recent times, with the advancement of computer technology, there is a significant increase in computational power. This makes the RANSE simulation to be the preferred practice at the initial stage of propeller design.

Due to the great promise RANSE method has shown, researchers and authors have frequently used it in recent times to estimate propeller open water characteristics. Funeno (2002) simulated fluid flow around a highly skewed propeller via unstructured mesh. For steady and unsteady flow, simulated results have good correspondence with experimental data. However, this process proved difficult and time-consuming. Marti nez-Calle *et al.* (2002) studied the numerical analysis of propeller via $k$-$\epsilon$ turbulence method in steady state condition. Although the results were satisfactory, the predicted torque coefficients were around 30% error. Watanabe *et al.* (2003) simulated propeller via $k$-$\omega$ turbulence model in open water and steady-state condition. Propeller symmetry was used in this study and only one blade was simulated, comparing to the experimental test there was 15% of error. Saha *et al.* (2018) performed CFD simulation of a Wageningen B-series propeller and obtained the lowest percentage of error in $K_T$ and $K_Q$ was 13% compared with the results obtained from the empirical formulae. Trejo *et al.* (2007) performed numerical analysis of marine propeller using ANSYS CFX 11. A full model of the propeller and only one blade of that propeller were simulated respectively. Obtained result has less than 10% error in estimating thrust and torque coefficient. Mossad *et al.* (2011) provided a complete guideline for geometry generation, boundary conditions, setup, simulation, and problems to achieve accurate results using CFD for marine propeller analysis. Both $k$-$\epsilon$ and $k$-$\omega$ turbulence models were used in this study. It concluded that $k$-$\epsilon$ sometimes overestimates the propeller open water characteristics. Prokash and Nath (2012) investigated four-bladed Wageningen B-series propellers and numerically analyzed them using unstructured mesh. Parra (2013) indicated no correlation in the differences between RANS analysis and Lifting Line Theory and obtained good results even for a high advance ratio (up to $J=1$). Elghorab *et al.* (2013) suggested a suitable mesh model through grid convergence test.

Bahatmaka *et al.* (2018) investigated KP505 propeller by SST $k$-$\omega$ model and obtained best mesh configuration through grid convergence test which results in less than 2% error in thrust. Triet *et al.* (2018) carried out mesh sensitivity analysis based on Y+ value and suggested that $k$-$\epsilon$ turbulence model gives quite a good result except at a high advance ratio (above $J=0.7$). Kolakoti (2013) did a CFD analysis of a ship's bare hull, a controllable pitch propeller's open water analysis, and the flow characteristics of that propeller affixed to the same hull. The numerical result obtained from this study has 4% and 14% errors in thrust and torque coefficient respectively in the operational regime of the propeller. Fitriadhy *et al.* (2020) performed CFD analysis of propellers for different numbers of blades and found that three-blade propellers are most efficient within the advance coefficient ranging between 0.8-0.9. Boumediene *et al.* (2019) studied the flow around Seiun Maru highly skewed marine propeller in both steady and unsteady cases and obtained average error percentage of 4.18% and 6.04% for thrust and torque coefficients respectively. In unsteady case, they suggested bringing the inlet boundary closer to the propeller. Harish *et al.* (2015) performed static analysis on a 4-bladed B-series propeller which was modeled using PropCad. Analysis was done for different materials (aluminum, R glass, S2 glass, carbon epoxy) and results showed that aluminum propeller provides minimum deformation. Neeharika and Babu (2015) found that metallic propellers can be replaced by composite propellers due to enhanced performance within the operating range. Shreyash *et al.* (2020) established that by replacing a marine propeller with a composite material, a low-weight blade can be created and made with a strong load-carrying capability and increase in efficiency.

Yu *et al.* (2013) investigated Ka-series with a 19A duct by employing panel method and RANS code and concluded that RANS code produces a better result. Szafran *et al.* (2014) studied the effects of duct shape on ducted propeller and concluded that between conventional 19A nozzle and perspective NACA-73_4212 nozzle, 19A nozzle gives better performance. Razaghian and Ghassemi (2016) analyzed a conventional propeller and then same propeller was fitted with accelerating 19A and decelerating N32 duct. 19A duct improved propeller characteristics while N32 model had a negative effect at a lower advance coefficient. The study of Majdfar *et al.* (2017) about the effect of length and angle of 19A duct on the hydrodynamic performance of propeller found that

increase in duct length doesn't significantly change the thrust coefficient. Gaggero *et al.* (2012) designed ducted propeller with a decelerating type of duct and found reduced cavitation phenomenon. Du and Kinnas (2019) analyzed Ka4-70 propeller with a19A duct. Target thrust is achieved with a higher efficiency after a few iterations by coupling RANS code with nonlinear optimization method.

The research mentioned above mainly focused on numerical analysis of either conventional marine propeller or ducted propeller. For this purpose, they applied RANSE code and other CFD methods on different types of propellers and ducts. Various type of elements is used such as Tetrahedral, Quadrilateral, Hexahedral, and so on. Different mesh size and grid independence test is also carried out to produce an accurate result. In most cases, researchers have used small size prototype propeller for simulation purposes and validated their result by towing tank experiments or by already published experimental data. Further study employing the RANSE approach to forecast propeller open water properties would benefit greatly from these investigations. However, their focus was not on how conventional and ducted propeller performance varies over advance coefficient under the same set of constraints. Moreover, they hardly consider the effect of fluid flow around an actual ship size propeller and its time complexity for simulation.

In this research, a 3-bladed Wageningen B-series propeller is designed in an iterative process. After geometric modeling of the propeller, it is numerically analyzed using commercial ANSYS CFX software. The same propeller is then fitted with an accelerating 19A duct and numerically analyzed again.

## 2. Theoretical Framework

The thrust and torque coefficient of the Wageningen B-series propeller is expressed by following regression formulae.

$$K_T = \sum_{n=0}^{39} C_n \left(J\right)^{s_n} \left(\frac{P}{D}\right)^{t_n} \left(\frac{A_E}{A_0}\right)^{u_n} \left(Z\right)^{v_n} \tag{1}$$

$$K_Q = \sum_{n=0}^{47} C_n \left(J\right)^{s_n} \left(\frac{P}{D}\right)^{t_n} \left(\frac{A_E}{A_0}\right)^{u_n} \left(Z\right)^{v_n} \tag{2}$$

### 2.1 Hydrodynamic coefficient

Whenever a propeller with a diameter (***D***) rotates in a uniform flow with angular velocity (***ω=2πn***) and velocity of advance (***V_A***) it generates thrust and torque. The hydrodynamic characteristics of a propeller are the non-dimensional coefficients that describe the forces and moments acting on the propeller. These coefficients are the advance coefficient (***J***), the propeller thrust coefficient (***K_T***), torque coefficient (***K_Q***), and open water efficiency (***η_0***) which can be computed respectively as follows:

$$J = \frac{V_A}{nD};\ K_T = \frac{T}{\rho n^2 D^4} \tag{3}$$

$$K_Q = \frac{Q}{\rho n^2 D^5};\ \eta_0 = \frac{J}{2\pi}\frac{K_T}{K_Q} \tag{4}$$

Where ***T*** and ***Q*** are thrust and torque of the propeller

### 2.2 Governing equation of fluid flow

It is assumed that the fluid is incompressible. These equations can explain the three-dimensional flow of an incompressible viscous fluid:

- Continuity equation

$$\frac{\partial p}{\partial t}+\frac{\partial\left(\rho u_x\right)}{\partial x}+\frac{\partial\left(\rho u_y\right)}{\partial y}+\frac{\partial\left(\rho u_z\right)}{\partial z}=0 \tag{5}$$

- Conservation of momentum equation

$$\rho\left(\frac{\partial V}{\partial t}+V.\nabla V\right)=-\nabla p+\mu\nabla^2 V+\rho g \tag{6}$$

- Equation of Turbulent Kinetic Energy

$$\frac{\partial\left(\rho k\right)}{\partial t}+\frac{\partial\left(\rho k u_i\right)}{\partial x_i}=\frac{\partial}{\partial x_j}\left[\left(\mu+\frac{\mu_t}{\sigma_k}\right)\frac{\partial k}{\partial x_j}\right]+P_k+P_b-\rho\varepsilon-Y_M+S_k \tag{7}$$

- Equation of Energy Dissipation

$$\frac{\partial\left(\rho\varepsilon\right)}{\partial t}+\frac{\partial\left(\rho\varepsilon u_i\right)}{\partial x_i}=\frac{\partial}{\partial x_j}\left[\left(\mu+\frac{\mu_t}{\sigma_k}\right)\frac{\partial\varepsilon}{\partial x_j}\right]+C_{1\varepsilon}\frac{\varepsilon}{k}\left(P_k+C_{3\varepsilon}P_b\right)-C_{2\varepsilon}\rho\frac{\varepsilon^2}{k}+S_\varepsilon \tag{8}$$

## 3. Numerical Simulation

The numerical model already presented is applied to a three-bladed conventional propeller. Before the application of numerical code geometry of the propeller and duct must be created properly.

### 3.1 Geometric modeling

The propeller adopted here is the Wageningen B-series propeller. The optimal diameter and pitch ratio of the propeller for the given power and propeller rpm are found 1.82 m and 0.76 respectively through an iteration process using Eq. (1) and Eq. (2). Optimum value of advance coefficient is found as 0.36.

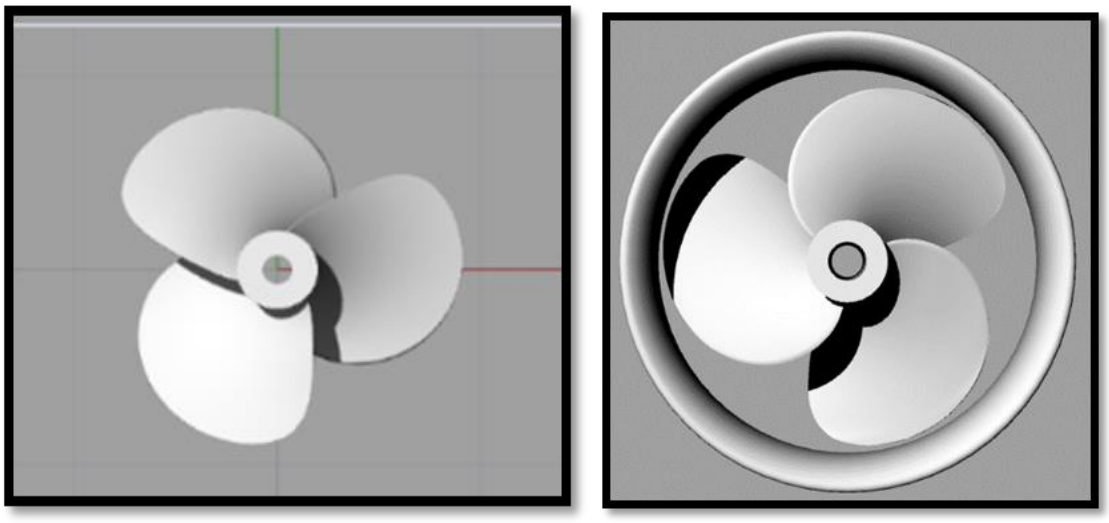

1(a): 3D propeller model (conventional) 1(b): 3D propeller model (Ducted)

Fig. 1: 3D model of conventional and ducted propeller

The coordinates of the Wageningen-B series propeller for the chosen design are calculated. Using the coordinates, 3D geometry is constructed in the plotting software PropCad. It has made geometry generation easier by considering easy setup of rake and skew angle. Again, this 3D geometry is further modified in the software Rhinoceros for the joining of the blades and hub, smoothing of the joints, etc. Fig. 1 shows final 3D model.

## 3.2 Mesh generation and boundary condition

Discretization of the rotary and static domain is done by FVM (Finite Volume Method). The domain sizes are specified in Fig. 2.

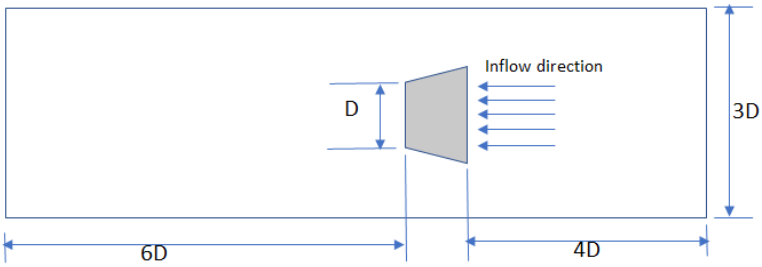


Fig. 2: Scheme for propeller and fluid domain

Both the stationary and rotary domains are cylindrical. The diameter of the stationary domain is 6D, the upstream length is 4D and the downstream length is 6D where D is the diameter of the propeller. The fluid will flow from upstream towards the trailing edge of the propeller. The Mesh element is tetrahedral. Both global and local meshing has been done. Local meshing has been applied at the propeller (in case of the ducted propeller in duct too) with a smaller cell size due to the complex shape of propeller to get better results. Quadratic order element, curvature capture (Minimum size: 10mm, Normal angle: 20˚), proximity capture (Minimum size: Globally 10mm and locally 5mm), Inflation (Maximum layer: 5, Growth rate: 1.2), Pitch tolerance (9mm), patch conforming method have been applied here. At global meshing, the element size is 200mm and it is 20mm at local meshing. A mesh convergence test has been performed for the conventional propeller.

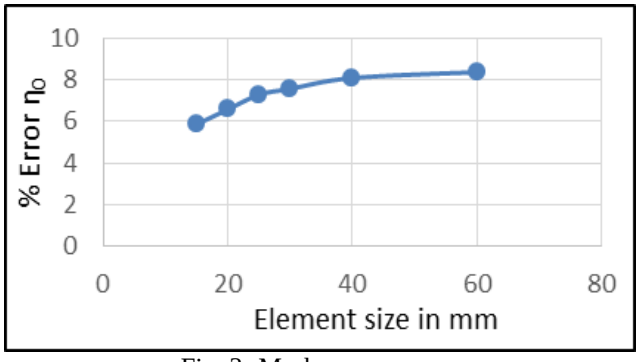


Fig. 3**:** Mesh convergence

Fig. 3 shows mesh convergence and Table 1 the result of mesh convergence test. Reduction in size of the element reduces the error percentage of open water efficiency. The least percentage of error is observed in element size 15 mm, but the simulation time is greater than in other element sizes. Since the result does not vary significantly after the reduction of element size below 25 mm, 20 mm element size has been chosen for simulation since it gives quite a reasonable error percentage in reasonable simulation time.

The meshing views of the conventional and ducted systems are shown in Fig. 4. For the conventional propeller system, the total number of elements is 1677098 and total number of nodes is 2341817. For the ducted propeller system, the total number of elements is 3180289 and total number of nodes is 4474012.

Three types of boundary conditions are used here. They are the velocity inlet, pressure outlet, and stationary wall on the propeller surface with no slip shear condition. In the case of ducted propeller, the duct is wall with no slip boundary condition.

Table 1: Mesh sensitivity analysis

| Element size (mm) | Total number of elements | % Error in $K_T$ | % Error in $10K_Q$ | % Error in $\eta_0$ |
|---|---|---|---|---|
| 15 | 1910315 | 4.4117 | 9.7078 | 5.8655 |
| 20 | 1677098 | 4.1578 | 10.0726 | 6.5773 |
| 25 | 1586888 | 3.7780 | 10.3093 | 7.2821 |
| 30 | 1546380 | 3.9821 | 10.7350 | 7.5650 |
| 40 | 1515127 | 3.8470 | 11.0408 | 8.0867 |
| 60 | 1502253 | 3.7629 | 11.1956 | 8.3698 |

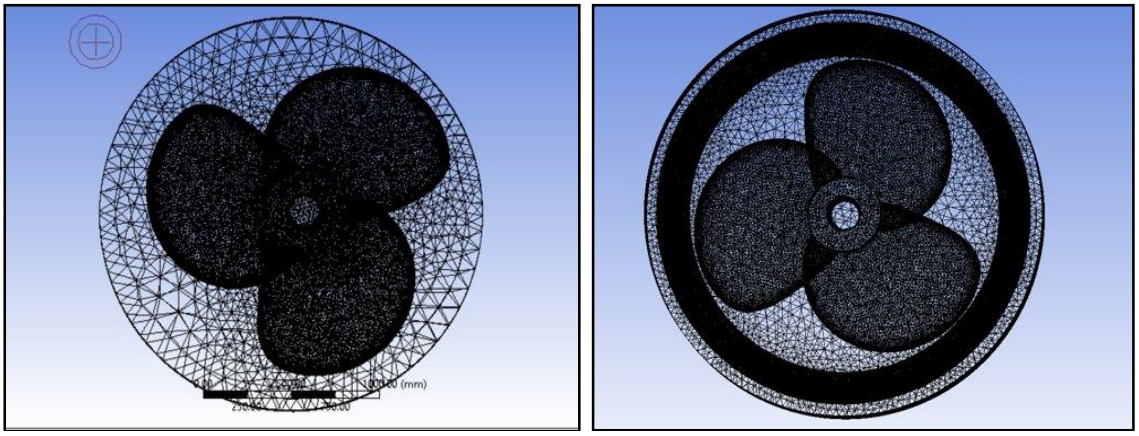

4(a): Conventional propeller meshing 4(b): Ducted propeller meshing

Fig. 4: Meshing of conventional and ducted propeller

## 3.3 Solver settings

The applied CFD code is ANSYS CFX. The RANS solver used here is pressure based with implicit formulation of linearization. The velocity formulation type is absolute, not relative and flow condition is not steady but transient. The viscous effect is considered as the ***k-ϵ*** realizable turbulence model is used. In the fluid zone, the frame motion has been applied where the propeller is stationary and the fluid rotates at an angular speed of 393 rpm. This is also referred to as a moving reference frame. SIMPLE algorithm has been chosen as the pressure-velocity method. Second order upwind discretization is used for momentum, turbulent kinetic energy, and turbulent dissipation rate, while second order downwind is used for pressure. Hybrid Initialization has been chosen as the initialization method. In the case of ducted propeller, instead of frame motion mesh motion is applied. The number of iterations and remaining amount varies simulation to simulation.

# 4. Results and Discussion

## 4.1 Conventional propeller

Open water diagram is plotted based on the data obtained from polynomial regression of Wageningen-B series propeller as shown in Fig. 5. Regression result shows that after ***J=0.8*** (approx.) thrust of conventional propeller becomes negative and the maximum efficiency is ***56%*** (approx.).

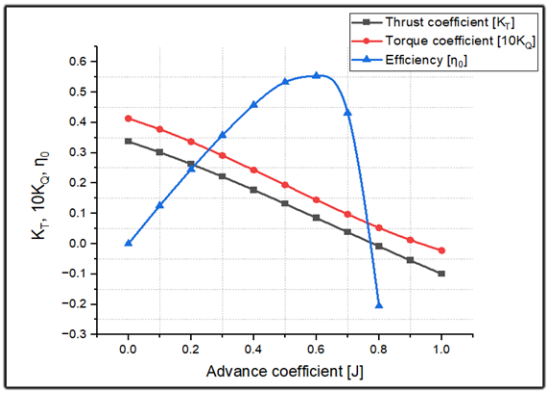


Fig. 5: Open water diagram of conventional propeller (Regression)

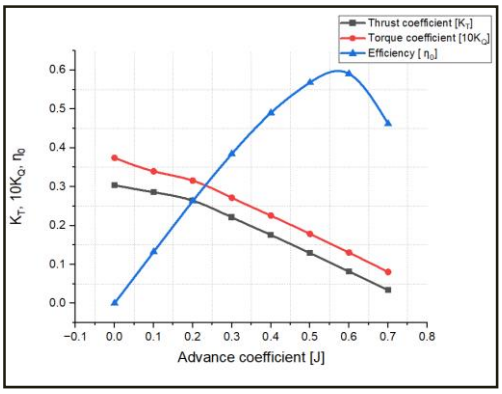


Fig. 6: Open water diagram of conventional propeller (Numerical)

Numerical analysis has been performed on this propeller and open water diagram is plotted using the data obtained from numerical analysis as shown in Fig. 6. Numerical result also shows that thrust is negative after ***J=0.7***. It provides a maximum efficiency of ***60%*** (approx.).

A comparison has been made between regression and numerical results in terms of percentage difference as shown in Table 2.

Table 2: Percentage difference between Theoretical and Numerical Analysis

| ***J*** | % $K_T$ | % $K_Q$ | % $\eta_0$ |
|---|---|---|---|
| .0001 | 9.8590 | 9.4799 | 0.4188 |
| 0.1 | 3.5041 | 8.4616 | -5.4157 |
| 0.2 | -0.4950 | 6.1777 | -7.1121 |
| 0.3 | -0.0224 | 6.8123 | -7.3344 |
| 0.4 | 0.8051 | 7.3060 | -7.0133 |
| 0.5 | 2.0277 | 8.0236 | -6.5189 |
| 0.6 | 4.1578 | 10.0726 | -6.5773 |
| 0.7 | 11.4879 | 17.1998 | -6.8984 |

The analysis is focused on advance coefficient up to ***J=0.7***. Within this range Table 2 indicates an acceptable level of percentage of error. In some cases, the percentage of errors is even lower than 1%.

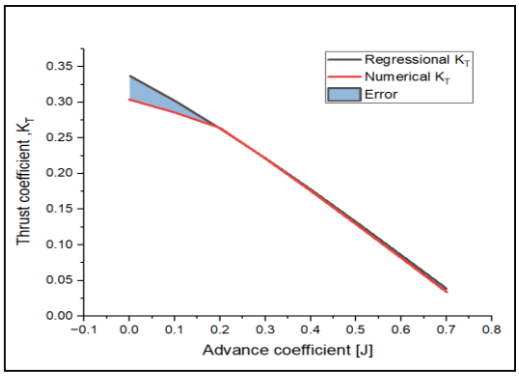


7(a): Error in thrust coefficient

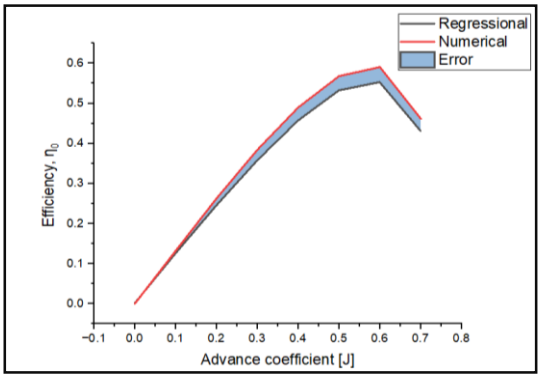


7(b): Error in efficiency

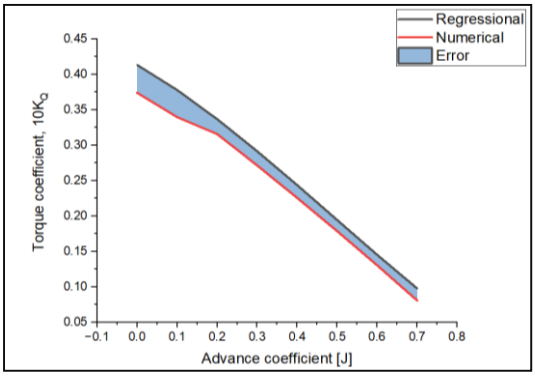


7(c): Error in torque coefficient

Fig. 7: Comparison of Numerical Analysis with Theoretical Result

A graphical representation of this comparison is shown in Fig. 7. From the comparison, it can be concluded that the efficiency obtained from the numerical result is giving slightly higher values than the regression result. The percentage error in thrust is much lower than error in torque and efficiency.

Table 3 shows that the error percentage in open water efficiency is 7.14% for the optimum condition.

Table 3: Error percentage for optimum value

| ***J*** | 0.3 | .36 | .4 |
|---|---|---|---|
| % $K_T$ | 0.02 | .49 | .81 |
| % $K_Q$ | 6.81 | 7.11 | 7.31 |
| % $\eta_0$ | 7.33 | 7.14 | 7.01 |

## 4.2 Ducted propeller

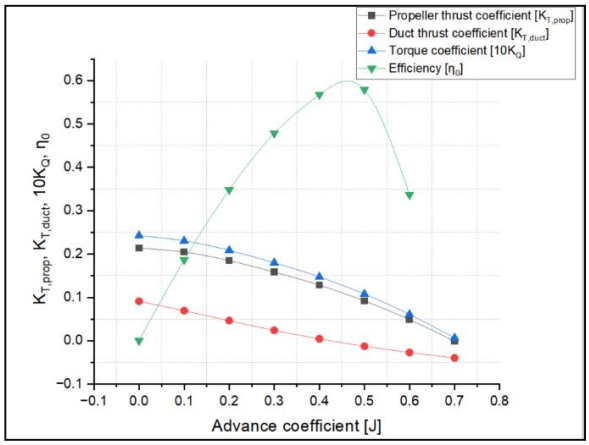


Fig. 8: Open water diagram of ducted propeller

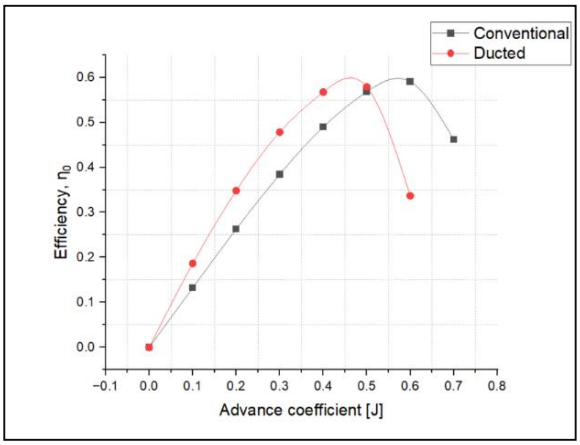


Fig. 9: Comparison between conventional and ducted propeller

Numerical analysis of ducted propeller shows that the thrust of the duct becomes negative from ***J=0.5*** which means as the speed increases, the performance of the duct decreases.

Fig. 8 shows that optimum efficiency is approximately 60% and the thrust of the propeller is always higher than the thrust of the duct.

### 4.3 Comparison

Furthermore, a comparison of efficiency has been made between the numerical results of the conventional propeller and ducted propeller as shown in Fig. 9.

This comparison shows that efficiency of ducted propeller increases as the advance coefficient increases. Efficiency of ducted propeller is highest at ***J=0.48*** (approx.) and service speed corresponding to this advance coefficient is 13 knots. For service speed higher than 13 knots, efficiency of the ducted propeller decreases significantly. Efficiency curves of ducted and conventional propeller intersect at ***J=0.5*** and service speed corresponding to this advance coefficient is 14 knots. For service speed above 14 knots, conventional propeller provides higher efficiency than ducted propeller. Therefore, both conventional and ducted propellers can be useful depending on the service speed of a particular vessel.

## 5. Conclusions

In this paper, conventional and ducted propellers were analyzed at different advance coefficients. Based on the numerical results following conclusions can be drawn:

- The open water characteristics of the conventional propeller are almost similar in case of regression and numerical analysis and there is an average 5.92% of error in efficiency.
- The maximum computed efficiencies for both the conventional and ducted propeller systems are found to be 60% but at different speeds.
- The ducted system provides better efficiency up to ***J=0.48*** and after that, the conventional system provides better performance. This conclusion can be drawn with more certainty if the ducted propeller can be tested in a towing tank or if numerical results can be verified by previously published experimental data.
- Accurate estimation of propeller hydrodynamic characteristics using CFD largely depends on the turbulence model, selected mesh type, and mesh density. ***k-ϵ*** realizable model with tetrahedral meshes of reasonable size can produce better result.
- The numerical results are intended to be more accurate estimates than prototype model tests since the propeller is simulated with actual size. The propeller performance is influenced by a variety of factors such as the effect of hull form, engine propeller matching and fouling after a certain operational period etc. So actual performance of a propeller can only be known after fully loaded service condition.

In future, various RANSE solver, different types of propellers and duct geometry can be studied. Additionally, if facility to experiment is accessible, towing tank experiment can also be done to verify the results of simulation.

## 6. Acknowledgements

The Department of Naval Architecture and Marine Engineering at BUET provided the essential tools for this research effort, for which the authors are grateful. They would like to express their gratitude to the anonymous reviewers whose comments helped to make this article better.

## 7. References

Bahatmaka, A., Kim, D. J., and Zhang, Y. (2018): Verification of CFD method for meshing analysis on the propeller performance with OpenFOAM, In 2018 International Conference on Computing, Electronics & Communications Engineering. https://doi.org/10.1109/iCCECOME.2018.8659085

Boumediene, K., Belhenniche, S., Imine, O., and Bouzit, M. (2019): Computational hydrodynamic analysis of a highly skewed marine propeller, Journal of Naval Architecture and Marine Engineering, 16(1), 21-32. https://doi.org/10.3329/jname.v16i1.38757

Du, W., and Kinnas, S. A. (2019, June): Optimization Design and Analysis of Marine Ducted Propellers by RANS/Potential Flow Coupling Method, In The 29th International Ocean and Polar Engineering Conference, OnePetro.

Neeharika, P. D,, and Babu, P. S. (2015): Design and analysis of ship propeller using FEA, In Proceedings of International Conference on Recent Trends in Mechanical Engineering.

Elghorab, M. A., Aly, A. A. E. A., Elwetedy, A. S., and Kotb, M. A. (2013): Open Water Performance Marine Propellers Using CFD, Research Gate.

Fitriadhy, A., Adam, N. A., Quah, C. J., Koto, J., and Mahmuddin, F. (2020): CFD prediction of b-series propeller performance in open water, CFD Letters, 12(2), 58-68. https://doi.org/10.22441/sinergi.2020.2.010
Funeno, I. (2002): On Viscous Flow around Marine Propellers-Hub Vortex and Scale Effect, Journal of the Kansai Society of Naval Architects, Japan, 2002(238), 17-27.
Gaggero, S., Rizzo, C. M., Tani, G., and Viviani, M. (2012): EFD and CFD design and analysis of a propeller in decelerating duct, International Journal of Rotating Machinery. https://doi.org/10.1155/2012/823831
Harish, B., Prasad, K. S., and Rao, G. U. M. (2015): Static Analysis of 4-Blade Marine Propeller, Journal of Aerospace Engineering & Technology, 5(2).
Kolakoti, A., Bhanuprakash, T. V. K., and Das, H. N. (2013): CFD analysis of controllable pitch propeller used in marine vehicle, Global Journal of Engineering Design and Technology, 2(5), 25-33.
Majdfar, S., Ghassemi, H., Forouzan, H., and Ashrafi, A. (2017): Hydrodynamic prediction of the ducted propeller by CFD solver, Journal of Marine Science and Technology, 25(3), 3.
Marti nez-Calle, J. N., Balbona-Calvo, L., Gonza lez-Pe rez, J., and Blanco-Marigorta, E. (2002): An open water numerical model for a marine propeller: A comparison with experimental data, In Fluids Engineering Division Summer Meeting, 36(169), 807-813. https://doi.org/10.1115/FEDSM2002-31187
Midoro, R., Musso, E., and Parola, F. (2005): (Maritime liner shipping and the stevedoring industry: market structure and competition strategies), Maritime Policy & Management, 32(2), 89-106. https://doi.org/10.1080/03088830500083521
Mosaad, M. A., MM, H., and Yehia, W. (2011): Guidelines for numerical flow simulation around marine propeller, In First International Symposium on Naval Architecture and Maritime, Istanbul.
Parra, C. (2013): Numerical investigation of the hydrodynamic performances of marine propeller, University of Galati, Gdynia, Master's thesis.
Perali, P., Lloyd, T., and Vaz, G. (2016): Comparison of uRANS and BEM-BEM for propeller pressure pulse prediction: E779A propeller in a cavitation tunnel, In Proceedings of the 19th Numerical Towing Tank Symposium, Nantes, France.
Prakash, S., and Nath, D. R. (2012): A computational method for determination of open water performance of a marine propeller, International Journal of Computer Applications, 58(12). https://doi.org/10.5120/9331-3636
Razaghian, A. H., and Ghassemi, H. (2016): Numerical analysis of the hydrodynamic characteristics of the accelerating and decelerating ducted propeller, Zeszyty Naukowe Akademii Morskiej w Szczecinie, 47 (119), 42-53.
Saha, G. K., Maruf, M. H. I., and Hasan, M. R. (2018): Marine propeller design using CFD tools, The Institution of Engineers, Bangladesh, 64.
Shreyash C. G., Aditya M. P., Shashank P. S. and Dheeraj K. A. (2020): Performance Analysis and Enhancement of Marine Propeller, International journal of engineering research & technology, 09(02). https://doi.org/10.17577/IJERTV9IS020020
Szafran, K., Shcherbonos, O., and Ejmocki, D. (2014): Effects of duct shape on ducted propeller thrust performance, Prace Instytutu Lotnictwa. https://doi.org/10.5604/05096669.1151026
Trejo, I., Terceno, M., Valle, J., Iranzo, A., and Domingo, J. (2007): Analysis of a ship propeller using cfd codes, Calculation of the resistance and the wave profile.
Triet, P. M., Thien, P. Q., and Hieu, N. K. (2018). CFD simulation for the Wageningen B-Series propeller characteristics in open-water condition using k-epsilon turbulence model, Science & Technology Development Journal-Engineering and Technology, 1(1), 35-42.
Watanabe, T., Kawamura, T., Takekoshi, Y., Maeda, M., and Rhee, S. H. (2003): Simulation of steady and unsteady cavitation on a marine propeller using a RANS CFD code, In Proceedings of The Fifth International Symposium on Cavitation.
Yu, L., Greve, M., Druckenbrod, M., and Abdel-Maksoud, M. (2013): Numerical analysis of ducted propeller performance under open water test condition, Journal of marine science and technology, 18(3), 381-394. https://doi.org/10.1007/s00773-013-0215-4